THE RELATIONSHIP OF MARINE STRATUS TO SYNOPTIC CONDITIONS

Donald Wylie, Barry Hinton, Peter Grimm
University of Wisconsin-Madison

Kevin Kloesel
The Pennsylvania State University

1. Introduction

The marine stratus which persistently covered most of the eastern Pacific Ocean, Had large clear areas during the FIRE Intensive Field Operations (IFO) in 1987. Clear zones formed inside the large oceanic cloud mass on almost every day during the IFO (Figure 1). The location and size of the clear zones varied from day to day implying that they were related to dynamic weather conditions and not to oceanic conditions. Forecasting of cloud cover for aircraft operations during the IFO was directed towards predicting when and where the clear and broken zones would form inside the large marine stratus cloud mass.

The clear zones often formed to the northwest of the operations area and moved towards it. However, on some days the clear zones appeared to form during the day in the operations area as part of the diurnal cloud burn off. The movement of the clear zones from day to day were hard to follow because of the large diurnal changes in cloud cover. Clear and broken cloud zones formed during the day only to distort in shape and fill during the following night.

The field forecasters exhibited some skill in predicting when the clear and broken cloud patterns would form in the operations area. They based their predictions on the analysis and simulations of the models run by NOAA's Numeric Meteorological Center. In this paper, we will discuss how the atmospheric conditions analyzed by one NOAA/NMC model related to the cloud cover.

2.Background

The forecasters knew before the IFO that the positions of the subtropical high at the surface and the upper air troughs could be used for predicting breaks and clear zones in the marine stratus. Clear and broken zones were observed prior to the IFO as upper air troughs reached the California coast. Clearing occurred when the trough axis crossed the coast moving east. At the surface, the subtropical high formed a nose that protruded into northern California (see Figure 2). Clear and broken zones often formed to the west of San Diego. When the subtropical high was farther offshore west of North America, the marine stratus cloud cover had fewer and smaller clear and broken areas.

After the FIRE IFO, we decided to quantify the relationship between the cloud cover and synoptic weather patterns. Before the IFO, we knew that the best meteorological information over the ocean was the analyses made for the model initializations by NOAA NMC. The surface analysis made by NOAA National Weather Service only pertained to continental conditions since few marine observations were available. The pressure patterns poorly depicted the subtropical high or the wind conditions observed offshore. Because of this problem, the forecasters exclusively used the NOAA/NMC model analyses for predicting wind directions and cloud cover changes.

3. Statistical Analysis of Model Fields

A statistical test was made to see if the model fields were related to marine stratus cloud cover. For this test, we extracted some standard dynamic and thermodynamic parameters from the model fields during the IFO. They were the 1000 mb wind components (U_{1000} and V_{1000}), temperature (T), dew point (T_d), dew point depression ($T-T_d$), 1000 mb height (Z_{1000}), 50 mb height (Z_{500}), 500 mb wind components (U_{500} and V_{500}), 1000 mb temperature advection ($V\bullet\nabla T$), and dew point advection ($V\bullet\nabla T_d$). Time series of these parameters were formed from the initial model fields at 00 and 12Z. The two values each day were averaged together to form a time series that could be correlated with one cloud cover analysis per day.

Seven locations in the eastern Pacific were chosen for this correlation test. They are shown in Figure 3. Each location was a grid point of the Global Circulation Model of NOAA/ NMC. At each location, cloud cover was defined as the fraction of a 100 line by 100 element box with brightness above two threshold levels on the GOES-West visible image at 20:00 Z (local noon). The two thresholds used were 15 counts (0-63 scale) for defining general cloud fraction and 30 counts for defining bright cloud fraction. These thresholds were arbitrarily chosen from a visual inspection of the images. An obvious brightness difference between cloud and clear could be seen on the images. We choose only images at local noon over a restricted part of the season to avoid the affects of changing illumination of the area. Cirrus and other cloud forms were absent during this 21-day period, so all satellite derived cloud cover fractions are indicative of marine stratus cloud cover.

These brightness levels tracked the changes in cloud cover for each box. The FIRE IFO aircraft flew in the general area of box 1. This area had nearly 100% cloud cover, except for three major clearing events. The cloud fraction in the box decreased after the first day. The lowest cloud fraction was reached on 4 July. Cloud cover rebuilt and a second major clearing event happened on 8 July. A decrease in bright cloud fraction occurred on 11 July with little change in the general cloud cover (lower brightness threshold). Nearly solid cloud cover followed until 18 July when a third major clearing event started and continued to the end of the IFO.

The difference between the cloud cover fraction at high and low brightness levels indicates the ranges in the pattern of the clouds on the satellite images. Cells or broken cloud patterns were present when the low brightness cloud fraction fell below 90%. This was indicative of cellular type clouds with nearly black areas in between. We assume the black areas were clear, However, higher resolution imagery form other satellites indicated that some small clouds were possibly present in these areas.

Cellular structure also was commonly observed when totally overcast conditions were present. These cells were bright spots inside solid cloud fields. The low brightness threshold cloud fraction was usually near 100% while the high brightness cloud fraction was lower. We generally interpret the low brightness cloud fraction as indicative of the general cloud cover while the high brightness cloud fraction followed the changes in bright cells. The bright cells being an indication of the more intense convection in the marine stratus.

A summary of our correlation between model fields and cloud fraction is given in Table 1. We had 21 days in our time series. A correlation of 0.36 was found to have a 90% confidence that a real correlation (non-zero) existed. These correlations are designated by the bold type in Table 1. We will note where correlations of this level or higher were found as being indicative of relationships.

U_{1000} and $V\bullet\nabla T_d$ correlated with cloud fraction in five out of seven boxes. Z_{1000} and T_d also had strong correlations in some boxes.

The relationships between $V \cdot \nabla T_d$ and cloud fraction also had one unusual factor. A negative correlation was found in five out of seven boxes. This indicated that cloud fraction increased with negative dew point advection ($-V \cdot \nabla t_d$), which would be expected. Negative dew point advection implies that advection is moistening the boundary layer. However, along the California coast in boxes 1 and 3 the opposite relationship was found, a positive correlation coefficient. This implied that cloud fraction decreased with ($-V \cdot \nabla T_d$) negative dew point advection. Boxes 1 and 3 appear to have other factors controlling marine stratus cloud formation. The dew points themselves (T_d) had very small correlations with cloud cover where as in the western boxes (5 and 7) the dew points had high correlations. Temperature advection ($V \cdot \nabla T$) correlations also followed the same signs as the dew point advection correlations in all boxes. This indicates the the cloud cover increased when advection attempted to lower the temperature and dew point along the northern California coast while to the west, the cloud cover decreased when advection acted to lower both T and T_d. The cloud cover obviously was controlled by different factors along the California coast than farther out in the open ocean. This difference is also evident by the high brightness cloud fraction. Boxes 1 and 3 had lower high brightness clouds fractions during most of the 21-day period than the other boxes. There was a general absence of bright cells in the marine stratus cloud fields. Boxes 1 and 3 are closer to the origin of the wind fetch acrossed the ocean. The marine stratus cloud fields had smaller and possibly thinner clouds while to the west in boxes 5 and 6. the cellular structure was better developed. Cloud top temperatures were also colder indicating a growth in cloud top heights. This is the area where marine stratus cloud fields began to transform into cumulus convective groups more closely related to trade wind cumulus. In the beginning of the wind fetch (boxes 1 and 3), the clouds may be related to mixing processes with the cold underlying ocean, a stable boundary layer situation. As the air moves southwest over warmer ocean temperatures, the boundary layer became less stable and more convection develops in the marine clouds.

4. Conclusion

Marine status cloud cover is predictable using NOAA NMC Global Circulation Model analyses. The forecasters observed patterns in the 1000 mb and 500 mb height fields that related to cloud cover changes. At the same time we have been able to statistically correlate atmospheric parameters analyzed by the model with observed cloud cover changes. This indicates that there is information in the model that can be used for parameterizing marine stratus clouds. The effects of these clouds on radiative heating and cooling can thus be developed.

Table 1: Correlation of the cloud cover defined by the low brightness threshold (15 counts on a 0-63 scale) with variables from NOAA/NMC's Global Model

	BOX NUMBER						
VARIABLE	1	2	3	4	5	6	7
Low vs High Brightness	**0.8**	**0.6**	**0.8**	**0.7**	**0.7**	**0.6**	**0.7**
$V \cdot \nabla T$	0.2	-0.3	0.3	-0.3	**-0.5**	-0.1	**-0.5**
$V \cdot \nabla T_d$	**0.5**	**-0.4**	**0.5**	-0.3	**-0.4**	-0.3	**-0.7**
Z_{1000}	**-0.4**	-0.2	0.0	0.3	-0.3	0.3	-0.2
Z_{500}	0.2	0.2	0.2	0.2	**0.4**	0.3	**0.6**

VARIABLE	BOX NUMBER 1	2	3	4	5	6	7
T	-0.1	-0.3	0.1	0.0	0.3	**0.4**	**0.6**
T_d	-0.0	-0.0	0.2	0.1	**0.8**	-0.0	**0.7**
$(T-T_d)$	-0.1	-0.1	-0.3	-0.1	**0.8**	0.3	**-0.5**
U_{1000}	0.3	0.2	**-0.4**	**-0.4**	**-0.5**	**-0.5**	**-0.7**
V_{1000}	0.1	-0.3	0.3	-0.3	-0.3	-0.1	-0.1

A

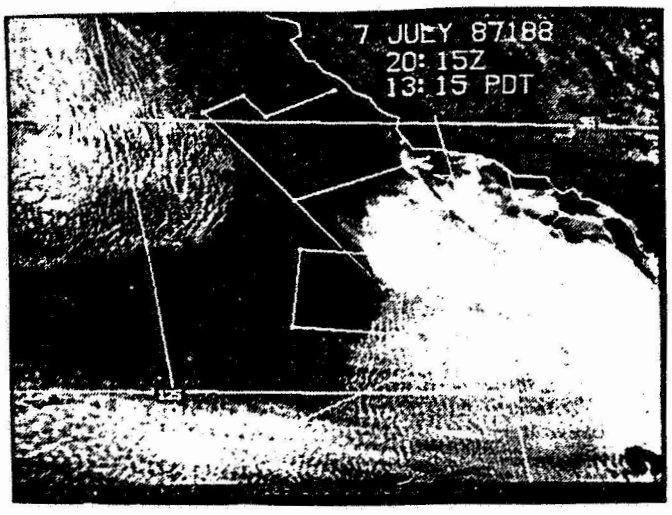

Figure 1

GOES satellite imagery for 7 July 1987.
(A) Visible 2015Z,

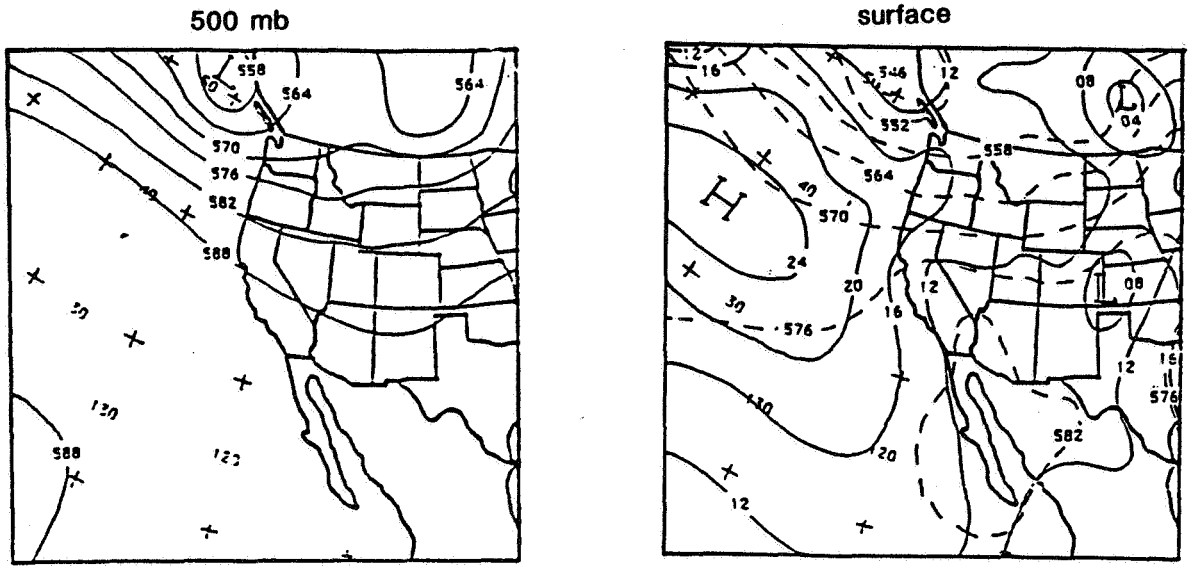

Figure 2: NGM analysis of surface pressure and 500 mb heights for 12:00 GMT 7 July 1987

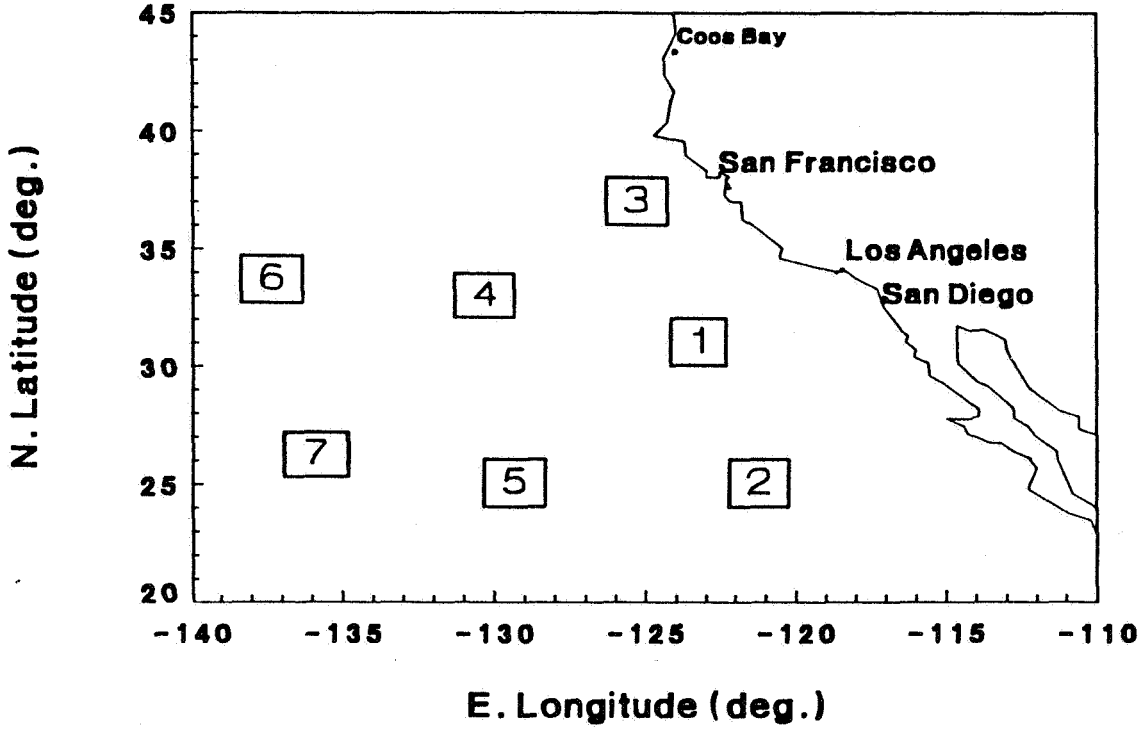

Figure 3: The locations of the boxes used in correlating cloud cover with atmospheric parameters shown in Table 1.